

Directional Biases in Back Trajectories Caused by Model and Input Data

Kristi A. Gebhart, Bret A. Schichtel, and Michael G. Barna

National Park Service, Air Resources Division, Cooperative Institute for Research in the Atmosphere, Colorado State University, Fort Collins, CO

ABSTRACT

Back trajectory analyses are often used for source attribution estimates in visibility and other air quality studies. Several models and gridded meteorological datasets are readily available for generation of trajectories. The Big Bend Regional Aerosol and Visibility Observational (BRAVO) tracer study of July to October 1999 provided an opportunity to evaluate trajectory methods and input data against tracer concentrations, particulate data, and other source attribution techniques. Results showed evidence of systematic biases between the results of different back trajectory model and meteorological input data combinations at Big Bend National Park during the BRAVO. Most of the differences were because of the choice of meteorological data used as input to the trajectory models. Different back trajectories also resulted from the choice of trajectory model, primarily because of the different mechanisms used for vertical placement of the trajectories. No single model or single meteorological data set was found to be superior to the others, although rawinsonde data alone are too sparse in this region to be used as the only input data, and some combinations of model and input data could not be used to reproduce known attributions of tracers and simulated sulfate.

IMPLICATIONS

Back trajectories are useful for assessments of the source regions that contribute to measured pollutant concentrations. However, the choice of back trajectory model and input meteorological data can influence the results of these assessments. Subtle deviations in predictions of transport direction are especially important to evaluate for receptors near political boundaries of interest and for those that are in or near areas of complex terrain, sparse meteorological measurements, or both. This study shows the value of evaluating the trajectories against the results of other analyses to determine which combination of trajectory model and input meteorological data yields the best results.

INTRODUCTION

Back trajectory analyses have been used routinely for at least two decades for qualitative and quantitative source attribution estimates in many air quality and visibility studies,^{1,2} and there is at least one example of a trajectory analysis being used to forecast visibility as early as the 1940s.³ In most of these visibility studies, both the trajectory model and the input meteorological data were coarse and simplistic by the standards today. However, within the past several years, newer trajectory models and increasingly sophisticated gridded input meteorological data have become more readily available.

There are several reasons to compare results from the various combinations of trajectory model and meteorological input data. First, one would like insight as to whether conclusions of older studies are still valid or are flawed and have biased results because of an inadequate model or input data. Second, because there are many possible combinations of trajectory models and input data, it is of interest to know how the different combinations manifest themselves and whether this affects the implication of source areas. Finally, although older models and coarser input data are generally assumed to produce poorer results, this has not always proven true. For example, in a tracer study at Grand Canyon National Park, the simplest back trajectory model performed slightly better than two prognostic mesoscale models.⁴ Also, more sophisticated models and data are more expensive in terms of complexity, time, effort, and computer resources. If simpler models produce similar results, then their ease of use and lower cost may justify their continued use. Stohl⁵ provides a relatively recent literature review and summary of some earlier analyses of trajectory accuracy.

The Big Bend Regional Aerosol and Visibility Observational (BRAVO) study^{6–9} was designed to examine causes of visibility impairment at Big Bend National Park (BBNP), located in Southwestern Texas on the Texas-Mexico border. One component of BRAVO was an intensive field measurement study that was conducted in Texas from

July to October 1999. These measurements provided researchers with a rare opportunity to evaluate several trajectory models, input meteorological data, and statistical analysis techniques against an extensive collection of field data, including fine particulate concentrations, upper level winds measured with radar wind profilers, and perfluorocarbon tracers released from four sites in Texas. Results from trajectory models can also be evaluated against results from regional air quality simulations performed for BRAVO.^{10,11}

BBNP is a particularly challenging receptor site for which to generate back trajectories because of its proximity to both complex terrain and the data-sparse regions of Mexico and the Gulf of Mexico. The earliest back trajectory analyses of BBNP date back to the mid-1980s when it was observed that high-particulate sulfur occurred mostly during September and October when trajectories arrived from the southeast and from areas in the United States extending back through Texas and Louisiana.¹² Another 1980s study of the areas of influence of major sulfur dioxide source regions in the Western United States¹³ found that sulfur at BBNP was influenced by sources in Northern Mexico, including the Monterrey region, the Arizona copper smelters (which have since substantially reduced emissions), and the Texas Gulf Coast. Back trajectory analyses of data collected during a Big Bend visibility study in 1996 found that sulfur and trace element concentrations were different for air masses from different regions.¹⁴ Sulfur was highest when transport was from the east and northeast including East Texas and areas farther upwind in the Eastern United States. Other regions associated with high sulfur were Northern Mexico and an area on the west coast of Mexico. Back trajectories were also used to investigate sulfur, organic carbon (OC), and soil at BBNP for 1989–1998.¹⁵ Again, sulfur typically peaked during summer and fall with high concentrations associated with transport from either Northern Mexico or East Texas and areas northeast of there. OC, usually highest in May, was largely because of agricultural burning in Mexico and Central America, while episodes of fine soil in July were because of Saharan dust. All of these studies relied on back trajectories generated with the 1980s-era Atmospheric Transport and Dispersion (ATAD) model¹⁶ with relatively coarse rawinsonde data as input.

In this study, back trajectories started from BBNP calculated in the historical method using ATAD are compared with those generated by the Hybrid Single-Particle Lagrangian Integrated Trajectory model (HYSPLIT)^{17,18} version 4.5 and the Center for Air Pollution Impact and Trends Analysis (CAPITA) Monte Carlo (CMC) model.¹⁹ Each trajectory model was run using at least three different gridded input meteorological data sets. Additionally,

ATAD was used as designed, with only standard rawinsonde data and rawinsonde data supplemented with data from four BRAVO radar wind profilers. Other BRAVO work⁶ compared the differences between the input meteorological datasets, whereas this study examines the resulting back trajectories.

INPUT METEOROLOGY

Rawinsonde Data

ATAD was designed to use standard twice-daily National Weather Service rawinsonde data. These data are available for 1946–1997 from the National Climatic Data Center²⁰ and for later years can be obtained from a website maintained by the Forecast Systems Laboratory of the National Oceanic and Atmospheric Administration (NOAA).²¹ Data include height, pressure, wind speed, wind direction, temperature, and dew point temperature. The archive consists of all of the observations transmitted via the North American Global Telecommunications Service (GTS), primarily from North and Central American civilian and some military rawinsonde sites. Since late 1998, the archive has been upgraded to include all international observations transmitted via GTS. All of the raw data goes through quality control analyses including gross error and hydrostatic consistency checks. At most sites, rawinsondes are launched twice daily at 12:00 a.m. and 12 UTC. There are generally one to three launch sites per state.

BRAVO Radar Wind Profilers

Data from four radar wind profilers⁶ deployed in Eastern and Southern Texas, at BBNP, Llano, Eagle Pass, and Brownsville from July to October 1999 as part of BRAVO were used to supplement the rawinsonde data for input to ATAD. These profilers measured hourly wind speed and direction as a function of height. Radar wind profilers equipped with a radio acoustic sounding system also obtained vertical profiles of virtual temperature, although usually only at heights of 500–1500 m. Wind profiler data were collected in two modes where the mode is the vertical resolution. The 60-m mode extends up to ~3300 m, and the 100-m mode reaches ~5000 m. Generally, the 60-m mode data are used for the lowest 700 mb, with the 100-m data used above that level.

Mesoscale Model

The Fifth Generation Penn State/National Center for Atmospheric Research Mesoscale Model (MM5) Version 3^{22,23} with four-dimensional data assimilation was run for BRAVO primarily to provide custom meteorological data fields for use in chemical air quality modeling. However, because it was available, the MM5 output also provided an

alternate modeled wind field to use as input for the trajectory models. The MM5 model was run in nonhydrostatic mode using a continental-scale 36-km domain with nested 12-km and 4-km domains. Only the 36-km output was used for trajectory modeling. At this scale, MM5 used analysis nudging to move the solutions toward an objective analysis of observed data. Table 1 summarizes the choices^{24–28} for some of the optional parameters in MM5. More details of the BRAVO MM5 modeling are summarized in a report.²³

Eta Data Assimilation System

The National Weather Service National Centers for Environmental Prediction (NCEP) maintains operational meteorological models for weather forecasting. One system is the Eta (now North American Mesoscale [NAM]) Data Assimilation System (EDAS).^{29,30} EDAS meteorological fields are generated using a three-dimensional variational objective data assimilation analysis scheme that uses the Eta/NAM forecast model to optimally merge and spatially interpolate measured meteorological fields. The Eta/EDAS system is continuously evolving, and some changes have been made since the BRAVO study. In 1999, EDAS incorporated 34 different data types from 26 data sets^{31,32} including land and marine surface observations, upper air data from the rawinsonde and wind profiler networks, the Aircraft Communications Addressing and Reporting System, and meteorological fields derived from satellite data.

In 1999, NCEP operated EDAS on a 32-km grid on a terrain-following vertical coordinate system with 45 levels and generated meteorological fields every 3 hr. These data were interpolated to a 40-km Lambert Conformal grid and isobaric levels. The NOAA Air Resource Laboratory (ARL)

saves a subset of the EDAS data suitable for input into dispersion models.¹⁸ In 1999, this archive contained the EDAS data with every other grid point saved on 22 isobaric surfaces for an effective 80-km grid spacing.

A fire at the NCEP computing facility on September 27, 1999, caused a month-long disruption in the availability of the EDAS data. For that reason, FNL data, described below, were used as input to the trajectory models instead of EDAS during October 1999. The input dataset called EDAS/FNL refers to a dataset consisting of EDAS when available (July–September 1999) with FNL substituted for October 1999.

FNL

The Global Data Assimilation System (GDAS)^{33–35} is another operational system that NCEP runs to generate inputs for meteorological forecast models. GDAS uses a spectral statistical interpolation (SSI) scheme coupled with the spectral Medium Range Forecast model.³⁶ The SSI scheme is closely related to the three-dimensional variational analysis system used in EDAS, and it incorporates similar data to EDAS. However, GDAS is the final run in the series of NCEP operational model runs and includes late-arriving data that can not be incorporated into EDAS.³⁷

NCEP runs GDAS four times a day at 00, 06, 12, and 18 UTC. Model output is for the SSI analysis time and a 6-hr forecast. The NCEP postprocessing of the GDAS converts the data to 1° latitude-longitude (360 × 181) grids and from the 42 σ level vertical coordinate system to isobaric levels. The NOAA ARL takes these fields and converts them to polar stereographic grids with ~180-km resolution and saves 13 pressure levels.^{18,38} Some fields, such as precipitation and surface fluxes, are only available

Table 1. Summary of optional parameters used to run MM5 for BRAVO.

Parameterization	Methodology	Reason
Initialization	Eta archived data supplemented with National Weather Service data and BRAVO profilers.	All reasonably available data were used
FDDA (36-km scale)	Analysis nudging with observed state estimated by temporal interpolation between analyses; Alapaty ¹⁹ adaptation for surface thermodynamic and moisture data; no temperature or moisture nudging in boundary layer	Assimilation of National Weather Service synoptic scale data; surface adaptation because of absence of high resolution soil moisture and temperature data
Convection	Kain-Fritsch ²⁰ deep-convection parameterization	Excellent performance for semiarid climates
Resolved cloud microphysics and precipitation	Dudhia ²¹ microphysics scheme	Most thoroughly tested; mixed-phase solutions found to add little benefit
Planetary boundary layer and turbulence	Shafran ²² 1.5-order turbulence scheme	Includes predictive equation for turbulent kinetic energy; most accurately represents surface temperatures and mixed-layer depths
Surface fluxes	Zhang-Anthes ²³ surface flux scheme	Two soil layers and predictive equation for ground temperature
Radiation	Dudhia ²¹ two-stream broad-band scheme	No reason given

at the forecast time, so ARL merges the GDAS and forecast runs to create a complete archive. Because GDAS is the last operational model run, it is known as the “final run” at NCEP, and ARL calls this archive FNL.

TRAJECTORY MODELS

ATAD

ATAD¹⁶ is a Lagrangian parcel model with one vertical layer. The vertical limits of the layer can be specified by the user, but the model default (used for BRAVO) is for the model to calculate a time-varying transport layer depth. The base of the layer is generally 300 m above the ground. For most time periods, the top of the layer is the lowest level within a critical inversion at which the potential temperature is 2 K above that at the inversion base. A critical inversion is defined as an inversion with a potential temperature lapse rate of at least 5 K/km. When no critical inversion exists, the transport layer top is assumed to be 3000 m above the ground. For trajectories that begin at night, the initial transport layer depth is approximated by $2\sigma_z$, where σ_z is the standard deviation of the vertical dispersion of a Gaussian plume for stable conditions calculated by $(2K_z t)^{1/2}$, where t is travel time and K_z is the vertical coefficient of eddy diffusion (1 m²/sec.) This is used only until the first daytime period of the trajectory.

Average winds within the transport layer are interpolated spatially (inverse of squared distance weighting) and temporally from all of the available data within 250 km. If there are no stations within 250 km, data within 600 km are used. The trajectory is terminated if there are no upper air data within that radius. Complex terrain is not explicitly considered in the model, although the transport layer is always ≥ 300 m above the terrain near each rawinsonde station. A back trajectory is started from the receptor every 6 hr. An air parcel position, or “endpoint,” is determined for every 3 hr backward in time for a maximum of 5 days. The gridded meteorological data, EDAS, FNL, and MM5, were used in ATAD by allowing the model to assume that each grid point was a rawinsonde site.

HYSPLIT

HYSPLIT^{17,18} was developed by the NOAA ARL. It can compute a range of outputs from simple air parcel trajectories to dispersion and deposition simulations. For BRAVO, the model was used in simple back trajectory mode. Version 4.7r is now available, but modeling for BRAVO was completed with version 4.5.

In its trajectory mode, HYSPLIT can do computations forward or backward in time. Default vertical motion, used for BRAVO, is to use the gridded input vertical motion data. HYSPLIT can be run with nested meteorological data and can use alternate vertical motion options, such as following isobaric or isentropic surfaces, but these were not considered

for this study. Required input is a gridded meteorological dataset with data at regular intervals. Back trajectory positions or endpoints are calculated hourly. For BRAVO, trajectories were started hourly and traced for up to 10 days.

The advection of a particle or puff is computed from the average of the three-dimensional velocity vectors at the initial position and at the first guess of the next position. Velocity vectors are linearly interpolated in both space and time. Trajectories terminate if they exit the model top, specified as 10 km above ground level (AGL) for BRAVO, but advection continues along the surface if they intersect the ground. The integration time step can vary during the simulation and is computed such that the advection distance per time step is < 0.75 of the meteorological grid spacing. HYSPLIT differs from the other two models in that a start height must be specified. For BRAVO, trajectories with start heights of 10, 100, 200, 500, 1000, and 2000 m AGL were generated.

CAPITA Monte Carlo

CMC¹⁹ is a particle dispersion model capable of simulating regional scale transport, transformation, and dry and wet removal of aerosols. In BRAVO, only the transport module was used. Dispersion is simulated by releasing multiple particles, which are then advected and diffused. Advection of the particles is accomplished by multiplying the mean three-dimensional wind vectors at the location of the particle by the time step. The mean wind vector is obtained from the input meteorological data. The gridded wind fields are interpolated to the position of the particle using bilinear interpolation in the horizontal and linear interpolation in the vertical and in time. Perfect reflection is assumed at the surface, but if a particle reaches the grid edge or top of the model domain, it is terminated. Vertical and horizontal diffusion are modeled separately. For particles below the mixing height, vertical diffusion is simulated by evenly distributing the particles between the surface and the mixing height. Particles enter or leave the layer as it grows or contracts. Parameterization of horizontal diffusion is by a random walk displacement where values are randomly picked from a Gaussian distribution with zero mean and standard deviation $\sqrt{2K\Delta t}$. K is the horizontal eddy diffusion coefficient and is a function of time of day, season, and location. For these back trajectory analyses, 20 particles were released from BBNP each hour with positions tracked hourly for up to 10 days. Backward trajectories are calculated by using a negative time step, which is equivalent to the adjoint of the advection-diffusion equation implemented in the CMC model.³⁹

Table 2 is a summary of the major differences between the three trajectory models, including some details of input choices for BRAVO.

Table 2. Summary of differences among three trajectory models used for BRAVO.

Feature	ATAD	HYSPLIT	CAPITA MC
Input data type	Designed for raw sounding data; gridded data or supplemental profiler data can also be used	Gridded meteorological data; BRAVO study used EDAS, FNL, and MM5 36 km	Gridded meteorological data; BRAVO study used EDAS, FNL, and MM5 36 km
Available input data	Raw soundings: 1946—present; EDAS and FNL: 1997—present; MM5 and BRAVO wind profilers: July—October 1999	EDAS and FNL: 1997—present; MM5: July—October 1999	EDAS and FNL: 1997—present; MM5: July—October 1999
Horizontal motion	Within the transport layer, average winds calculated from stations within a given radius	Input horizontal winds	Input horizontal winds
Trajectory start height	As run for BRAVO, depends on transport layer (see vertical motion)	Chosen by user, for BRAVO, 10, 100, 200, 500, 1000, 2000 m above ground.	Below mixing height
Vertical motion	Trajectory stays in a variable calculated transport layer, ~300–3000 m above ground; fixed vertical layers are also possible	For BRAVO, input vertical winds used to calculate transport; maximum 10-km height; other options are available	Random vertical motion in mixed layer, vertical motion by input data above
Trajectory start frequency	Maximum of four times per day at 0, 6, 12, and 18 UTC	Hourly at multiple heights	Unlimited particles per hour (used 20–50 for BRAVO applications)
Frequency of output	Every 3 hr	Hourly* number of start heights	Hourly* number of particles per start time
Trajectory length	Maximum 5 days	For BRAVO 5, 7, and 10 days	For BRAVO 5, 7, and 10 days

TEST METHODS AND RESULTS

Comparisons of Individual Trajectories

As a first step, we graphically examined the horizontal and vertical locations of back trajectories generated by each model/data combination for each day of the BRAVO study. All of the trajectories were traced for 5 days backward in time from BBNP (103.18°W, 29.30°N). Several general observations resulted.

On some days, all of the trajectories are similar, and, thus, the choices of model, input data, and even start

height are unimportant. This is more likely during the fall than during summer. A common pattern, especially in the summer, is that there is a directional difference between trajectories generated by different methods. Figure 1 shows examples of some of the trajectories arriving at BBNP on July 19 and illustrates typical directional differences observed frequently during July and August. All of the model and input data combinations had air parcels arriving from the southeast across the Gulf of Mexico. Among them, the ATAD trajectory with rawinsonde input

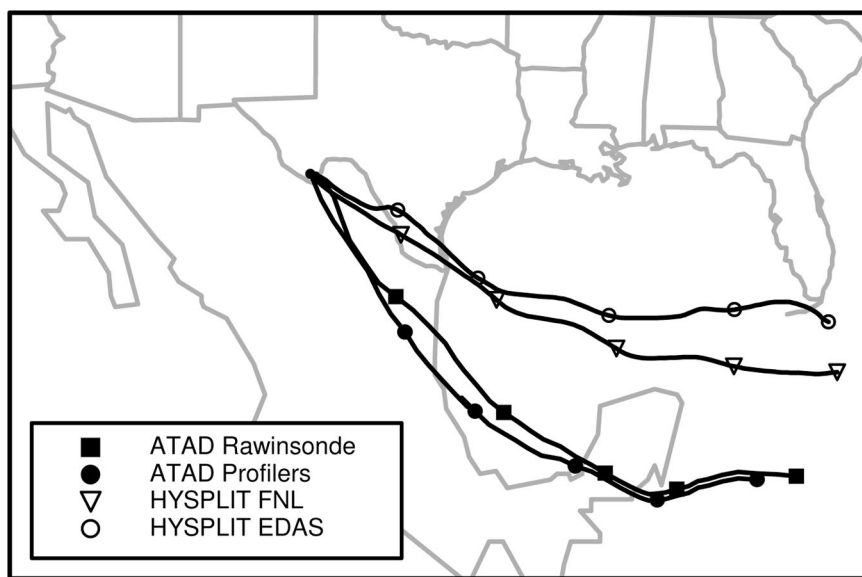


Figure 1. Illustration of common variations that occurred between trajectories started at the same time during July and August. This example shows 5-day back trajectories generated by four model/input combinations beginning on July 19, 1999 at 12:00 a.m. Central Daylight Time. The HYSPLIT trajectories were started at 100 m AGL. "ATAD Profilers" refers to ATAD with input from the standard rawinsonde network plus four BRAVO radar wind profilers.

arrived from the most southerly direction, whereas trajectories generated by HYSPLIT using EDAS generally were from the most northerly, and HYSPLIT with FNL or MM5 were often between these extremes. ATAD trajectories generated with a gridded wind field were more similar to HYSPLIT trajectories than ATAD trajectories generated with rawinsonde input, and CMC trajectories generated using EDAS input also arrived from a more northerly direction than those generated with MM5 input. Another common result is that the CMC trajectories generated with EDAS input usually had less horizontal spread than those generated using MM5; for example, if 20 particles were started from BBNP at a given hour, there was less horizontal difference between the 20 CMC back trajectories if EDAS was input than if MM5 was used. This was true even when the heights were similar. One explanation for this is that the coarser EDAS/FNL grids resolve less of the advection fluctuations than the MM5 grid.^{40,41}

For HYSPLIT, which requires specification of a start height, the height differences between individual trajectories started at the same height, but generated with EDAS versus FNL can be as large as several thousand meters after 5 days. Directional differences between trajectories generated by HYSPLIT using EDAS versus FNL can occasionally be as much as 180° and, as expected, are largest when trajectory height differences are large, although directional differences between trajectories from different input wind fields can exist even when the heights are similar. Trajectories generated with either HYSPLIT or CMC can reach as high as 10 km, clearly above the mixed layer that is likely to be carrying air pollutants. An advantage of CMC over HYSPLIT version 4.5 is that the height of the mixed layer is known and available as output. Though the most recent version of HYSPLIT can output the mixing height and several other variables, this was not available in version 4.5. CMC estimates transport integrated throughout the mixed layer, and ATAD does not generate trajectories above its “transport layer” or a maximum of ~3 km, so these models are less sensitive to height.

From this simple analysis, it was apparent that there can be significant episodic differences between the modeled back trajectories depending on model and input data. These observations are examined in a more systematic manner in the following section.

Study-Average Comparisons

Heights and Wind Speeds. It is evident from the individual trajectories that trajectory height can have a large influence on horizontal placement, and, on average, the greater the height, the faster the speed. This has implications for source attribution, because higher wind speeds will tend to implicate more distant source regions. Table 3 shows the mean endpoint heights and wind speeds for all

of the model and input data combinations. The highest HYSPLIT trajectories were with EDAS/FNL input with the largest data-dependant height differences at the lowest start heights. For start heights ≥ 200 m AGL, mean trajectory heights were approximately equal with either FNL or MM5 input, and for start heights of 1000–2000 m, all three input data sets gave approximately equivalent HYSPLIT trajectory heights.

Similarly, the highest trajectories from ATAD were with EDAS/FNL or rawinsonde input. FNL or MM5 input gave lower ATAD trajectories. In the CMC model, EDAS/FNL and MM5 input resulted in approximately equivalent mean heights.

A HYSPLIT start height of 500–1000 m most closely matches the mean heights generated by ATAD and CMC, which do more averaging within the mixed layer. Start heights of 200 m and greater in HYSPLIT (with some exceptions) usually resulted in mean trajectory heights approximately equal to the start height. For lower start heights, the mean trajectory height was not lower than 200 m with EDAS/FNL or MM5 input. FNL input did result in lower mean heights for lower start heights.

Overall Residence Times. Overall residence time (ORT),^{1,2,12,15} a count of the number of back trajectory endpoints or particles in each grid cell showing the predominant direction(s) from which air masses arrived, were calculated using 0.5° latitude by 0.5° longitude grid cells for July–October and for several subsets of the study period using 5-day and 10-day back trajectories generated with each model/dataset. While the analysis of individual trajectories made it apparent that there were occasional differences between the model/input combinations, ORT allows evaluation of the study-average differences between trajectories.

Differences Caused by Start Heights. HYSPLIT, which does less vertical averaging than ATAD and does not use the random vertical movements of CMC, is the most sensitive to start height. This is especially true if different start heights fall within different vertical layers of the input data. The start height needs to be situated so that trajectories represent the bulk of the air movement within the mixed layer. The average ORTs for the 4-month study period have subtle differences for slight changes in start heights. The lowest start heights generated a very small fraction of endpoints in the Western United States, and for the EDAS/FNL input there were very few end points in Mexico west and southwest of BBNP. The fractions of end points in these areas increase as the start heights increase. The most different pattern is for the 2000-m start height, which, for both EDAS/FNL and MM5, results in the most endpoints west of BBNP in both Mexico and the United States. Because trajectories started this high are, on average,

Table 3. Mean end point heights and wind speeds for 5-day back trajectories for July to October 1999 generated by all of the model and input data combinations.

Model	Input Data	Start Height (m AGL)	Mean Endpoint Height ^a (m AGL)	Mean Wind Speed (m/sec)
ATAD	Rawinsonde	NA	861	5.3
	Rawinsonde + BRAVO profilers	NA	863	5.4
	EDAS/FNL	NA	859	6.2
	FNL	NA	591	5.9
	MM5	NA	628	6.9
CMC	EDAS/FNL	NA	1156	6.2
	MM5	NA	1164	7.0
HYSPLIT version 4.5	EDAS/FNL	10	238	4.6
		100	364	5.0
		200	447	5.3
		500	706	5.8
		1000	1240	6.2
		2000	2617	6.9
		100–1000	686	5.6
		10	33	4.1
		100	134	4.6
		200	225	5.0
FNL	EDAS/FNL	500	495	5.8
		1000	1204	6.6
		2000	2451	6.9
		100–1000	515	5.4
		10	238	5.0
		100	252	5.1
		200	288	5.2
		500	462	5.3
		1000	950	5.4
		2000	2009	5.5
MM5	EDAS/FNL	100–1000	487	5.3

Note: A HYSPLIT start height of 100–1000 refers to an average of the results from 100, 200, 500, and 1000 m start heights. EDAS/FNL input refers to use of EDAS when available with FNL substituted for October; ^aFor ATAD, the mean end point height is estimated by half the mean transport layer depth.

above the mixed layer, they were not used for additional analyses. Also, trajectories started at 10 and 100 m were very similar and deemed redundant. The remaining start heights, 100, 200, 500, and 1000 m, all generate trajectories that are, on average, within the mixed layer, and these were aggregated for source attribution analyses in BRAVO.

Differences Caused by Input Data. ORTs for July–October 1999 generated by ATAD, using four different input data sets, were compared. Results for the two most different combinations are shown in Figure 2. Rawinsonde input alone results in trajectories arriving from the most southerly direction. Adding any additional data, even data from the four BRAVO profilers, caused ATAD to move the predominant wind direction more easterly, resulting in a southeasterly as opposed to a southerly average transport direction, with the largest easterly component being when EDAS/FNL input was used. MM5 and FNL input

give trajectories between the southerly (rawinsonde) and southeasterly (EDAS/FNL) extremes. The southerly bias in ATAD with rawinsonde input is apparently caused by the sparseness of the data in this region, so trajectories generated by this combination of model/input data for BBNP are suspect. Although the differences are subtle, for this receptor site they may make the difference between attributing pollutants to Mexico and attributing them to sources in the United States.

Consequences of FNL versus EDAS during October 1999. The EDAS wind field is assumed to be superior to FNL because of its finer horizontal, vertical, and temporal resolution. We would like to estimate the effect of substituting FNL for EDAS during October 1999, which was a quarter of the BRAVO study period.

Trajectories generated by ATAD and HYSPLIT using EDAS versus FNL input were generated for five Octobers:

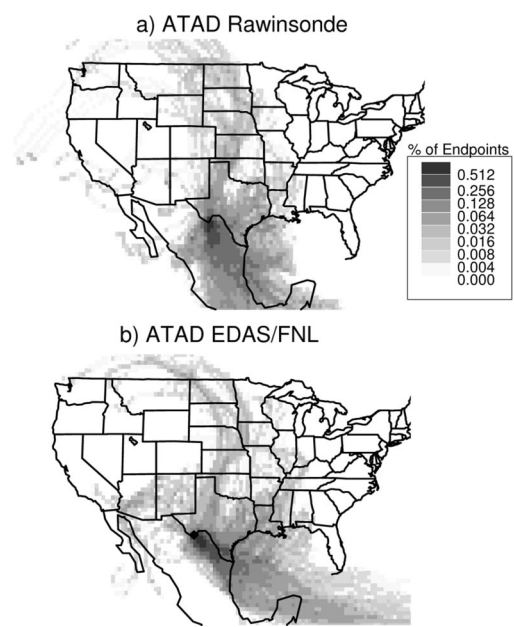


Figure 2. ORT for BBNP July to October 1999 using the ATAD model. (a) with rawinsonde data as input; (b) with EDAS/FNL input.

1997, 1998, and 2000–2002. The EDAS trajectories were substantially higher, sometimes twice as high on average, as those generated using FNL. ORTs were generated for each of the four trajectory sets and the differences compared. Figure 3 shows ORT differences between pairs of inputs for each model. The yellow-to-red colors illustrate where EDAS-generated trajectories were more likely to have endpoints, and the blue-to-green areas show where FNL-generated endpoints were more likely. EDAS input with either model was more likely to result in trajectories from southwest of BBNP, and, with HYSPLIT, EDAS also resulted in more trajectories from the northwest, especially Arizona. Conversely, FNL input in either model generated more end points in East Texas and more in Northwest Mexico. Also, consistent with the previous analyses, lower heights were associated with fewer endpoints in the Western United States. Because some interannual variability is expected, it is not possible to quantify the actual differences during October 1999. However, because October trajectories were aggregated with those

from July to September, and air masses from the west generally had low sulfate concentrations, the effect of using FNL rather than EDAS for the BRAVO source attribution of sulfate was probably not large.

Differences between Models. Another issue is how similar are the outputs from the three models when identical input data sets are used. Figure 4 shows the BRAVO 4-month average ORT generated by ATAD, CMC, and HYSPLIT, all using MM5 input. Similar graphs were generated for EDAS/FNL data. For both inputs, results from ATAD and CMC were the most similar, whereas the predominant wind direction from HYSPLIT was less southerly and more along the Texas-Mexico border.

Qualitative Tracer Tests

Perfluorocarbon tracers^{6–9} were released from four different sites during the second half of the BRAVO field study: Eagle Pass (250 km from BBNP), San Antonio (450 km), Houston (750 km), and Northeast Texas (750 km). During the first half of the study, three of the four tracers were released from Eagle Pass as “timing” tracers with release rates specified to determine transport times from Eagle Pass to BBNP, and the fourth was released from Northeast Texas. Several analyses can take advantage of the tracer data to help determine the accuracy of back trajectories. Trajectories should indicate a transport pathway between the tracer-release site and the receptor when the tracer concentration is high. However, this was not always the case. All of the model and wind field combinations were able to correctly locate the release sites at Eagle Pass and San Antonio on the days of the highest concentrations of tracers released there. None did well with the Northeast Texas tracer, although CMC and HYSPLIT with MM5 came closest. For the day with the maximum Houston tracer, CMC with either input and ATAD with all of the inputs except MM5 correctly passed over the release site, whereas HYSPLIT with either FNL or MM5 input produced trajectories that were too far north. All days of high Houston tracer concentrations were during October when EDAS data were missing.

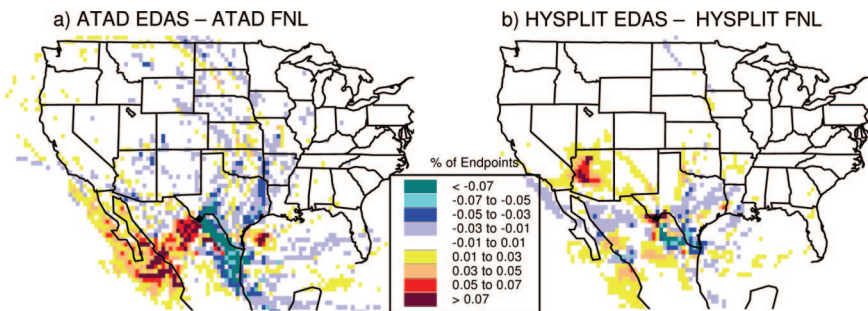


Figure 3. ORT differences during Octobers 1997, 1998, and 2000–2002. (a) ATAD/EDAS-ATAD/FNL; (b) HYSPLIT EDAS-HYSPLIT FNL.

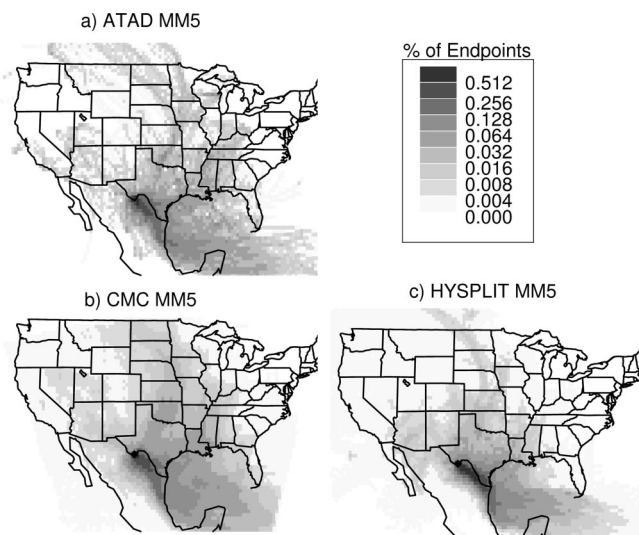


Figure 4. ORT s for July to October 1999 all with 36-km MM5 input (a) ATAD; (b) CAPITA MC; (c) HYSPLIT started at 100, 200, 500, and 1000 m AGL.

The differences between the 4-month high-concentration residence time^{1,2,12,14,15} (HRT) and the ORT for each of the tracers were also generated. HRT is similar to ORT, except it uses only trajectories that arrived on days with "high" concentrations. A high concentration was defined to be the 80th percentile or higher at BBNP. Peak (HRT-ORT) differences should occur over the tracer release site or at least along the transport pathway between there and the receptor. Again, there was not a single model or a single input field that uniformly performed better for all four of the tracers. All of the combinations did reasonably well for Eagle Pass and San Antonio. Conversely, most combinations were unable to generate peak residence time differences in the vicinity of the Northeast Texas release site. The two combinations that did best were ATAD with either EDAS/FNL or MM5 input. For the Houston tracer, any model with EDAS/FNL input did reasonably well, and ATAD with MM5 performed moderately well. In general, when model/wind field combinations missed the correct release site, all of the combinations tended to miss in the same direction. For Eagle Pass, those combinations that did less well were too southerly (or too clockwise). For San Antonio and Houston, respectively, the trajectories tended to either be correct or be too far to the northwest (or too counterclockwise).

Quantitative Tests

Two quantitative tests were used to determine how well back trajectories could reproduce known source attributions. BRAVO data sets that can be used for this purpose are the perfluorocarbon tracer concentrations apportioned to the tracer release sites and model-simulated sulfate apportioned to large source regions. Both

MM5 and EDAS/FNL wind fields can be tested using the tracers. For the simulated sulfate, only the MM5 dataset was tested, because that is what was used by the chemical air quality model, and, therefore, it is the meteorological reality for the simulation. The simulated sulfate allows testing of trajectories for source areas beyond Texas and for a depositing secondary pollutant. All three of the back trajectory models were tested in both cases.

In both tests, a simple linear regression model, trajectory mass balance (TrMB)^{6-9,42-44} was used to apportion the concentrations. In TrMB, the dependent variable is a vector of daily concentrations at the receptor, and the independent variables are the number of back trajectory endpoints in each of several preselected source areas. Figures 5 and 6 show the source areas used for the TrMB tests for the tracers and simulated sulfate, respectively.

Tracer. Daily total tracer concentrations were calculated by summing the concentrations of the individual tracers for each day during September 17–October 28, 1999 (42 days), when they were released from four different sites. The fraction caused by each tracer is the fraction arriving from its release site. The Northeast Texas tracer was eliminated, because although there were episodes when high concentrations of this tracer were detected at BBNP, the mean concentration was near zero.

Table 4 summarizes the results of the tracer test. Several model and data combinations were able to reproduce the known attributions of all of the tracers to within the errors in the measurements and the standard errors of the regression coefficients. These included HYSPLIT with EDAS/FNL, CMC MM5, ATAD MM5, and ATAD rawinsonde. Trajectories of 5-, 7-, and 10-day lengths were examined, but there was little difference relative to the duration of the trajectory; this is expected, because the release sites are, on average, <5 days away. The worst

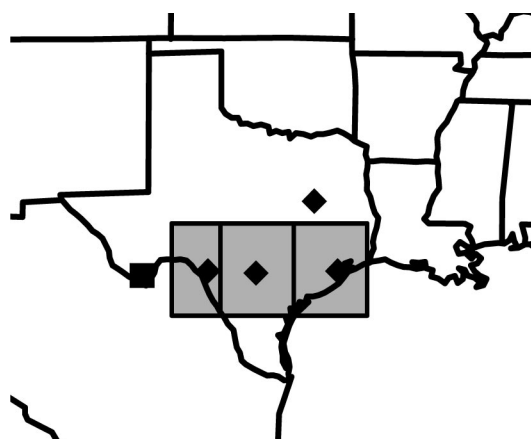


Figure 5. BBNP (■), perfluorocarbon tracer release sites (◆) and TrMB source areas used to model tracer concentrations.

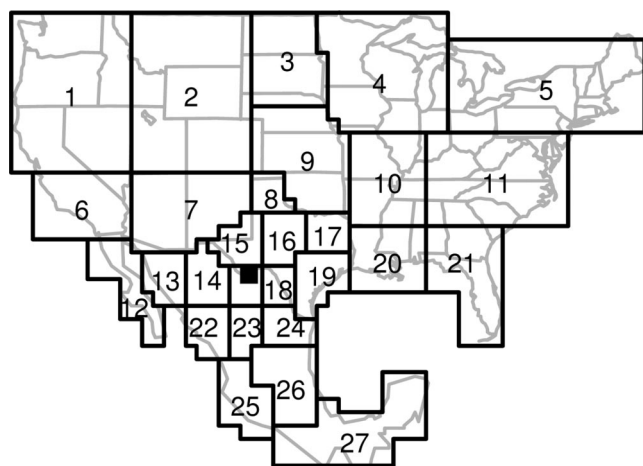


Figure 6. Numbered boxes are the 27 source areas used in the TrMB regressions for sulfate. Western United States is 1–3, 6, 7, and 9; Eastern United States is 4, 5, 10, 11, 20, and 21; Texas is 8, 15–17, and 19; Mexico is 12–14, 18, and 22–27. The black square is BBNP.

performance was exhibited in the HYSPLIT MM5 combination, which dramatically overpredicted the Eagle Pass contribution and underpredicted San Antonio. Eagle Pass is ~250 km southeast of BBNP, whereas San Antonio is almost twice as distant, at ~450 km. Other poorly performing combinations were ATAD EDAS/FNL and CMC EDAS/FNL, which both overestimated the Houston contribution and underestimated San Antonio. Houston is the most distant of the three release sites at ~750 km, so these latter combinations overestimated the most distant source area. Based on the correlations between individual pairs of source areas and a variance inflation test⁴⁵ for multicollinearity, the problems with the underperforming combinations were unrelated to collinearity between

source areas. The remaining two possibilities for error are either the tracer concentrations or the trajectories. These and other BRAVO analyses^{6–9} indicate that the tracer values were reasonably accurate to within their reported uncertainties. This leaves the placement of the back trajectories within Texas as the only possibility for error. Therefore, results from this tracer evaluation suggest that although all model and input data combinations produced trajectories that appeared adequate for qualitative analyses, trajectories generated by HYSPLIT MM5, CMC EDAS/FNL, and ATAD EDAS/FNL were inadequate to quantitatively distinguish source areas within Texas during BRAVO.

Simulated Sulfate. Table 5 summarizes the attributions of REMSAD-modeled sulfate^{6–11} to each of the four large BRAVO source regions, the Eastern United States, the Western United States, Texas, and Mexico, as shown in Figure 6. Similar comparisons were not done for the smaller individual areas, because REMSAD results for all of them were not calculated. For purposes of this test, there is no assertion that the simulated sulfate concentrations or attributions from REMSAD are accurate; rather, the approach is to determine which trajectory model can best estimate the same sulfate concentrations and source attributions as the air quality model, given that both simulations are using the same MM5 wind field. The REMSAD-simulated source attributions explicitly include emissions, deposition, and chemistry, whereas the trajectory-based regression model estimates only the study-long mean influence of these factors. The dependent variable in the trajectory-based regressions was the simulated, not the measured sulfate. Values within 10 percentage points of the “correct” answer

Table 4. Results of TrMB modeling of three BRAVO tracers at BBNP for September 17–October 28, 1999 (42 days).

Variable	Eagle Pass	San Antonio	Houston	R ²
Mean Concentration (ppq)	0.155 ± 0.024	0.559 ± 0.081	0.062 ± 0.008	NA
Mean Percent (%)	20 ± 4	72 ± 13	8 ± 1	NA
ATAD Rawinsonde 5-day	35 ± 12	65 ± 14	0 ± 9	0.495
ATAD EDAS/FNL 5-day	16 ± 8	33 ± 9	51 ± 9	0.708
HYSPLIT EDAS/FNL 5-day	28 ± 12	67 ± 13	5 ± 9	0.640
CAPITAMC EDAS/FNL 5-day	30 ± 9	43 ± 10	27 ± 8	0.721
ATAD MM5 5-day	34 ± 12	60 ± 13	6 ± 9	0.564
HYSPLIT MM5 5-day	82 ± 18	18 ± 18	0 ± 11	0.484
CAPITAMC MM5 5-day	23 ± 16	77 ± 19	0 ± 12	0.643

Note: The first three rows show the tracer release sites, the mean measured concentrations, and the percentage of the total measured concentration attributable to each tracer. Remaining rows give the modeled percent attributions. Those that are accurate to within the uncertainty of the measurement and standard error of the regression coefficients are shown in bold and a larger font for easy identification.

Table 5. Percent attributions of predicted REMSAD sulfate by TrMB for July 6 to October 28, 1999 (115 days), using MM5 winds.

Model	Texas (%)	Mexico (%)	Eastern United States (%)	Western United States (%)	R ²	Mean Overpredicted SO ₄ (ng/m ³)	Mean % Overprediction
REMSAD ('correct')	18	25	46	10	1.000	0	0
CAPITAMC 5-day	19	31	39	11	0.778	-23	-1%
CAPITAMC 7-day	20	24	36	20	0.798	-12	-1%
CAPITAMC 10-day	21	21	37	21	0.775	-13	-1%
HYSPLIT 5-day	43	25	16	17	0.768	11	+1%
HYSPLIT 7-day	43	23	16	18	0.820	-26	-1%
HYSPLIT 10-day	46	21	19	13	0.801	-14	-1%
ATAD 5-day	25	33	36	8	0.735	-24	-1%

Note: Values in the top row are the REMSAD attributions with the boundary conditions (7%) and nonlinear components (2%) proportionally redistributed. TrMB attributions within 10 percentage points of the REMSAD attributions are shown in larger font bold type. The last three columns are statistics comparing the TrMB predictions to 'observed' (REMSAD predicted) sulfate concentrations.

are highlighted in the table. "Correct" was defined as the REMSAD attributions with boundary conditions (7%) and nonlinear attributions (2%) proportionally redistributed to the remaining source areas. The best performance in terms of matching the REMSAD and back trajectory attributions was with the CMC MM5 combination using 5-day trajectories, although the 7-day and 10-day trajectories were nearly as good. ATAD MM5 also attributed sulfate correctly to all four of the source regions within 10% of the correct values. HYSPLIT MM5 was able to reproduce the correct attributions for Mexico and the Western United States but was unable to correctly apportion sulfate from Texas and the Eastern United States, attributing much more to Texas and much less to the Eastern United States than REMSAD.

Lengths of 5, 7, or 10 days in CMC made little difference in the predictions except for the Western United States, which is predicted to be the source of twice as much sulfate with 7- or 10-day trajectories as with 5-day lengths. This is intuitively reasonable, because air masses rarely arrived at BBNP directly from the Western United States but more often traversed across the Eastern United States and/or Texas before arrival. Thus, on average, the travel time from the Western United States was longer than from the other large source areas.

Why is HYSPLIT not accurately reproducing the attributions when it uses essentially the same input meteorological data as CMC and ATAD? A large difference between CMC and HYSPLIT occurs on September 1. This is also the day of the highest sulfate concentration at BBNP and, hence, is an influential point in the regression. Although CMC and ATAD place most of the endpoints in the Eastern United States on this day, HYSPLIT places most of them in Texas. All of the trajectories have the same general direction, but the HYSPLIT trajectories are much lower in height and, in fact, are essentially on the

ground. This is true even for those started at 1000 m. Because of the lower height, they also have much lower wind speeds and thus remain in Texas, while CMC and ATAD trajectories extend into the Eastern United States. Because this was an influential day, the differences in trajectory heights on this day alone may explain why HYSPLIT was unable to reproduce the REMSAD source attributions. EDAS and FNL wind fields were not evaluated using the method described above, because REMSAD only used the MM5 input wind fields to generate the simulated sulfate.

Biases at Big Bend during Other Seasons and Years

All of the analyses to this point are valid only for BBNP during July to October 1999. Differences between models and wind fields may be quite different during other years, other seasons, and at other receptor sites. MM5 data and BRAVO wind profiler data are not readily available for other time periods. However, it is possible to examine differences between seasonal ORTs as generated in previous studies by ATAD and those generated by HYSPLIT and its most readily available input data, EDAS and FNL. Figure 7 shows the ORT for each season for 1997–2002 for each of these combinations. Winter is defined as December, January, and February, and so forth. For consistency, 1999 was eliminated from all of the fall analyses because of the missing EDAS data in October 1999. For summer, the biases of 1999 appear to be consistent with other years. ATAD is the most southerly, HYSPLIT EDAS the most easterly, and HYSPLIT FNL falls between the two. During all other seasons, the major difference between ATAD and HYSPLIT is that HYSPLIT with either EDAS or FNL input has more trajectories arriving from the west. This indicates that previous analyses based only on

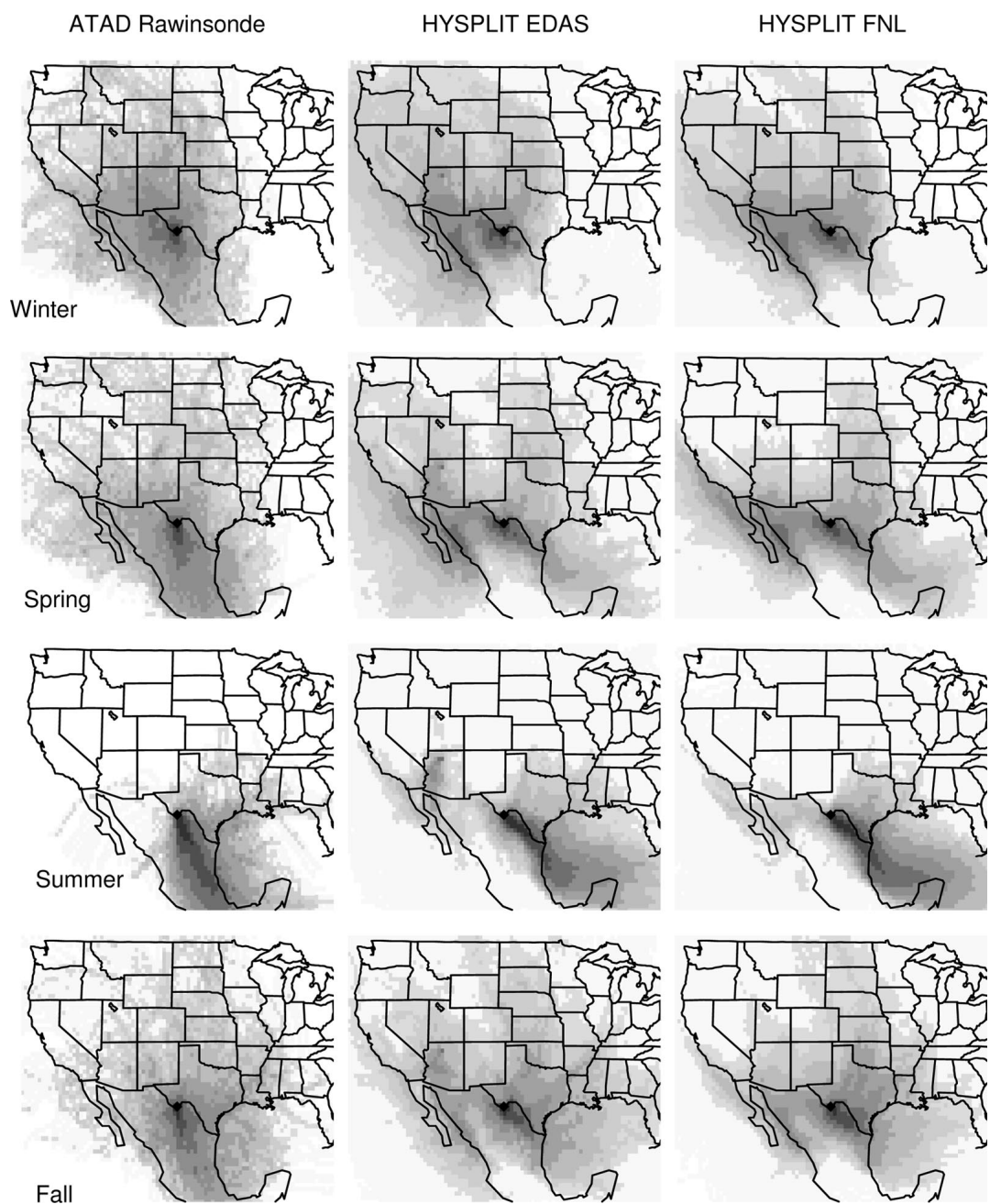


Figure 7. ORTs for 1997–2002 by season and using ATAD with rawinsonde data, HYSPLIT with EDAS data, and HYSPLIT with FNL data. HYSPLIT results include start heights of 100, 200, 500, and 1000 m AGL. Fall does not include 1999. Scale is the same as in Figures 2 and 4.

ATAD^{12–15} may have underestimated the transport from Northwestern Mexico and Arizona. Also, as in the examination of EDAS versus FNL for Octobers, the fall ORTs again show that HYSPLIT EDAS puts more endpoints in Arizona than HYSPLIT FNL.

Biases at Other Receptor Sites

ORT comparisons similar to those discussed above for BBNP were also generated for Grand Canyon National Park, AZ, and Great Smoky Mountains, TN, for an indication of whether similar differences in back trajectories also exist for other parts of the country and whether conclusions drawn from BRAVO can be extrapolated to

other sites and seasons. Differences between model/input sets were smallest at Great Smoky Mountains. The largest differences at that site were in the spring when ATAD had more trajectories arriving from the northeast than HYSPLIT, which had more from the northwest. At Grand Canyon, differences were small for all seasons for the predominant wind direction (air masses from the southwest). The largest differences were during the winter, when ATAD was more likely to have trajectories from the northeast, while HYSPLIT had more from the southeast. On an annual average, HYSPLIT EDAS has more trajectories from the southeast than either HYSPLIT FNL or ATAD

at both Grand Canyon and Great Smoky Mountains. Results for other sites are not discussed in detail here but, in general, are different enough from the results for BBNP that it is likely that differences between models and wind fields in other regions may be different from what was observed at BBNP during BRAVO.

DISCUSSION AND CONCLUSIONS

Analyses of back trajectories by several methods showed evidence of systematic differences between the average results of different back trajectory model and meteorological input data combinations at BBNP during the BRAVO field study of July to October 1999. On individual days, especially during the fall, all of the trajectories, regardless of model and input choices, are often similar, but for some individual episodes, trajectories generated by different methods can be very different, even by as much as 180°. On average, trajectories generated with EDAS data arrived from the most easterly direction, whereas output from ATAD with rawinsonde input generated trajectories from the most southerly areas. Trajectories generated using MM5 and FNL input fell between these extremes. Most of the differences were caused by the input meteorological data rather than the trajectory model, although there were also some differences attributable solely to the model when the same input data were used. Model differences are primarily caused by the different mechanisms used for vertical placement of the trajectories. These findings corroborate an earlier study of trajectory accuracy that also found that major factors contributing to trajectory differences were variations in input data and in the treatment of vertical motion by the models.⁴⁶

HYSPLIT is the most sensitive to horizontal start location, start height, and subsequent placement of individual endpoints, because small changes in endpoint position can affect the grid cell and vertical layer for which data are used for the next time step. Small differences in trajectory height can sometimes result in large differences in horizontal placement of trajectories. Differences caused by occasional shifting of an endpoint from one grid cell and/or horizontal layer to a neighboring one are minimized when trajectory data are aggregated over many start times and/or start heights. Aggregation of trajectories over several nearby horizontal starting points, although not done for BRAVO, would also help minimize this sensitivity. Start heights in HYSPLIT affect the mean trajectory height and, hence, mean speed. For BRAVO, mean trajectory heights from HYSPLIT were usually approximately equal to the start height. Mean trajectory heights from CMC and ATAD were insensitive to start height and were approximately equivalent to those from HYSPLIT with 500–1000-m start heights. HYSPLIT and ATAD with EDAS/FNL input generated higher trajectories

than with MM5 input. Mean trajectory heights by CMC were approximately the same with either MM5 or EDAS/FNL input. ATAD is the least sensitive to horizontal location of the start point.

Qualitative tests of whether trajectories could correctly find four perfluorocarbon tracer release sites in Texas were inconclusive. None of the trajectory models or input meteorological fields was clearly superior to the others.

A quantitative linear model was used to test the ability of different back trajectories to reproduce known source attributions. HYSPLIT EDAS/FNL, CMC MM5, ATAD MM5, and ATAD with rawinsonde data were able to approximately reproduce tracer attributions for source areas within Texas. A similar test of simulated sulfate could only be run using MM5 data. In this case, CMC MM5 and ATAD MM5 performed better than HYSPLIT MM5.

Cursory examination of trajectory differences for other regions and other seasons indicates that the magnitude of the directional differences between the models and wind fields is both geographically and seasonally dependent, and the direction of these biases cannot necessarily be inferred from the BRAVO data. Previous trajectory-based analyses of BBNP data using ATAD with rawinsonde input likely overestimated the impact of Mexican sources during the summer. During other seasons, the older studies may have underestimated transport from Northwestern Mexico and Arizona, but emissions in those regions are relatively low, so resulting errors in source attribution were likely inconsequential. The summer southerly bias by ATAD with rawinsonde input is caused by the sparse meteorological data in this region.

DISCLAIMER

The assumptions, findings, conclusions, judgments, and views presented herein are those of the authors and should not be interpreted as necessarily representing official National Park Service policies.

REFERENCES

1. Ashbaugh, L.L.; Malm, W.C.; Sadeh, W.Z. A Residence Time Probability Analysis of Sulfur Concentrations at Grand Canyon National Park. *Atmos. Env.* **1985**, *19*, 1263–1270.
2. Poirot, R.L.; Wishinski, P.R. Visibility, Sulfate and Air Mass History Associated With the Summertime Aerosol in Northern Vermont; *Atmos. Env.* **1986**, *20*, 1457–1469.
3. Miller, J.E.; Mantis, H.T. An Objective Method of Forecasting Visibility; *Bull. Am. Meteor. Soc.* **1948**, *29*, 237–250.
4. Green, M.C.; Pai, P.; Ashbaugh, L.; Farber, R.J. Evaluation of Wind Fields Used in Grand Canyon Visibility Transport Commission Analyses: *J. Air & Waste Manage Assoc.* **2000**, *50*, 809–817.
5. Stohl, A. Computation, Accuracy and Applications of Trajectories: A Review and Bibliography; *Atmos. Env.* **1998**, *32*, 947–966.
6. Schichtel, B.A.; Gebhart, K.A.; Barna, M.G.; Malm, W.C.; Day, D.; Kreidenweis, S.; Green, M. Big Bend Regional Aerosol and Visibility Observational (BRAVO) Study Results: Air Quality Data and Source Attribution Analyses Results from the National Park Service / Cooperative Institute for Research in the Atmosphere; Final Report, July 2004; available at http://vista.cira.colostate.edu/improve/Studies/BRAVO/reports/FinalReport/bravofinalreport_CIRA.htm (accessed October 6, 2005).

7. Pitchford, M.L.; Tombach, I.H.; Barna, M.G.; Gebhart, K.A.; Green, M.C.; Knipping, E.; Kumar, N.; Malm, W.C.; Pun, B.; Schichtel, B.A.; Seigneur, C. Big Bend Regional Aerosol and Visibility Observational Study (BRAVO) Study. Official Report of the sponsoring agencies: U.S. Environmental Protection Agency, National Park Service, Texas Commission on Environmental Quality, EPRI, and National Oceanic and Atmospheric Administration. 2004; available at <http://vista.cira.colostate.edu/improve/Studies/BRAVO/reports/FinalReport/braovofinalreport.htm> (accessed October 6, 2005).
8. Schichtel, B.A.; Pitchford, M.; Gebhart, K.A.; Malm, W.C.; Barna, M.G.; Knipping, E.M.; Tombach, I.H. Reconciliation and Interpretation of Big Bend National Park's Particulate Sulfur Source Apportionment: Results from the BRAVO Study. Part I; *J. Air & Waste Manage. Assoc.* **2005**, *55*, 1709-1725.
9. Pitchford, M.L.; Schichtel, B.A.; Gebhart, K.A.; Barna, M.G.; Malm, W.C.; Tombach, I.H.; Knipping, E.M. Reconciliation and Interpretation of the Big Bend National Park's Particulate Light Extinction Sulfate Source Apportionment: Results from the BRAVO Study. Part II; *J. Air & Waste Manage. Assoc.* **2005**, *55*, 1726-1732.
10. Barna, M.G.; Gebhart, K.A.; Schichtel, B.A.; Malm, W.C. Modeling Regional Sulfate during the BRAVO Study: 1. Base Emissions Simulation and Performance Evaluation; *Atmos. Env.* In review.
11. Barna, M.G.; Schichtel, B.A.; Gebhart, K.A.; Malm, W.C. Modeling Regional Sulfate during the BRAVO Study: 2. Emission Sensitivity Simulations and Source Apportionment; *Atmos. Env.* Submitted for publication.
12. Bresch, J.F.; Reiter, E.R.; Klitch, M.A.; Iyer, H.K.; Malm, W.C.; Gebhart, K.A. Origins of Sulfur-Laden Air at National Parks in the Continental United States. In *Proceeding of the Transactions of the Air Pollution Control Association Specialty Conference: Visibility Protection—Research & Policy Aspects*; Bhardwaja, P.S., Ed.; 1986; pp 695-708.
13. Malm, W.C.; Gebhart, K.A.; Henry, R.C. An Investigation of the Dominant Source Regions of Fine Sulfur in the Western United States and Their Areas of Influence; *Atmos. Env.* **1990**, *24a*, 3047-3060.
14. Gebhart, K.A.; Malm, W.C.; Flores, M. A Preliminary Look at Source-Receptor Relationships in the Texas-Mexico Border Area; *J. Air & Waste Manag. Assoc.* **2000**, *50*, 858-868.
15. Gebhart, K.A.; Kreidenweis, S.; Malm, W.C. Back-Trajectory Analyses of Fine Particulate Matter Measured at Big Bend National Park in the Historical Database and the 1996 Scoping Study; *Sci. Tot. Env.* **2001**, *276*, 185-204.
16. Heffter, J.L. Air Resources Laboratory Atmospheric Transport and Diffusion Model (ARL-ATAD), National Oceanic and Atmospheric Administration, Technical Memo, ERL-ARL-81; National Oceanic and Atmospheric Administration: Washington, DC, 1980.
17. Draxler, R.R.; Hess, G.D. An Overview of the HYSPLIT_4 Modeling System for Trajectories, Dispersion, and Deposition; *Aust. Meteo. Mag.* **1998**, *47*, 295-308.
18. READY (Real-Time Environmental Applications and Display System); NOAA Air Resources Laboratory; available at <http://www.arl.noaa.gov/ready/hysplit4.html> (accessed October 6, 2005).
19. Schichtel, B.A.; Husar, R.B. Regional Simulation of Atmospheric Pollutants with the CAPITA Monte Carlo Model; *J. Air & Waste Manag. Assoc.* **1997**, *47*, 331-343.
20. Schwartz, B.E.; Govett, M.A. Hydrostatically Consistent North American Radiosonde Data Base at the Forecast Systems Laboratory, 1946-Present; NOAA Technical Memorandum ERL FSL-4; National Oceanic and Atmospheric Administration/Environmental Research Laboratories/Forecast Systems Laboratory: Boulder, CO, 1992.
21. Govett, M. National Oceanic and Atmospheric Administration-Forecast Systems Laboratory, Radiosonde Database Access; available at <http://raob.fsl.noaa.gov> (accessed October 6, 2005).
22. Grell, G.A.; Dudhia, J.; Stouffer, D.R. A Description of the Fifth Generation Penn State/National Center for Atmospheric Research Mesoscale Model (MM5); NCAR Technical Note (TN-398-STR); National Center for Atmospheric: Boulder, CO, 1994.
23. Seaman, N.L.; Stouffer, D.R. Final Report to EPRI Contract EP-P3883/C1886 for MM5 Modeling in Support of the Big Bend Regional Aerosol and Visibility Observation Study (BRAVO); The Pennsylvania State University for Electrical Power Research Institute: Palo Alto, CA; Available at http://vista.cira.colostate.edu/improve/Studies/BRAVO/reports/FinalReport/BRAVO/A9_Seaman2003MM5Modeling.pdf (accessed October 6, 2005).
24. Alapaty, K.; Seaman, N.L.; Niyogi, D.S.; Hanna, A.F. Assimilating Surface Data to Improve Accuracy of Atmospheric Boundary Layer Simulations; *J. Appl. Meteo.* **2001**, *40*, 2068-2082.
25. Kain, J.S.; Fritsch, J.M.A. One-Dimensional Entrainment/Detraining Plume Model and Its Application in Convective Parameterization; *J. Atmos. Sci.* **1990**, *47*, 2784-2802.
26. Dudhia, J. Numerical Study of Convection Observed during the Winter Monsoon Experiment Using a Mesoscale Two-Dimensional Model; *J. Atmos. Sci.* **1989**, *46*, 3077-3107.
27. Shafran, P.C.; Seaman, N.L.; Gayno, G.A. Evaluation of Numerical Predictions of Boundary-Layer Structure During the Lake Michigan Ozone Study (LMOS); *J. Appl. Meteor.* **2000**, *39*, 412-426.
28. Zhang, D.L.; Anthes, R.A.A. High-Resolution Model of the Planetary Boundary Layer-Sensitivity Tests and Comparisons with SESAME-79 Data; *J. Appl. Meteor.* **1982**, *21*, 1594-1609.
29. Black, T.L. The New NMC Mesoscale Eta Model: Description and Forecast Examples; *Wea. Forecasting* **1994**, *9*, 265-278.
30. Parrish, D.; Purser, J.; Rogers, E.; Lin, Y. The Regional 3D Variational Analysis for the Eta Model; In *Proceedings of the 11th Conference on Numerical Weather Prediction*; American Meteorological Society: Norfolk, VA, 1996; pp 454-455.
31. Zapotocny, T.H.; Nieman, S.J.; Menzel, W.P.; Nelson, J.P. III; Jung, J.A.; Rogers, E.; Parrish, D.F.; DiMego, G.J.; Timothy, M.B.; Schmit, J.A. Case Study of the Sensitivity of the Eta Data Assimilation System; *Wea. Forecasting* **2000**, *15*, 603-621.
32. Zapotocny, T.H.; Menzel, W.P.; Nelson, J.P. III; Jung, J.A. An Impact Study of Five Remotely Sensed and Five in Situ Data Types in the Eta Data Assimilation System; *Wea. Forecasting* **2002**, *17*, 263-285.
33. Kanamitsu, M. Description of the NMC Global Data Assimilation and Forecast System; *Wea. Forecasting* **1989**, *4*, 335-342.
34. Derber, J.C.; Parrish, D.F.; Lord, S.J. The New Global Operational Analysis System at the National Meteorological Center; *Wea. Forecasting* **1991**, *6*, 538-547.
35. Parrish, D.F.; Derber, J.C. The National Meteorological Center's Spectral Statistical Interpolation Analysis System; *Mon. Wea. Rev.* **1992**, *120*, 1747-1766.
36. Sela, J.G. Spectral Modeling at the National Meteorological Center; *Mon. Wea. Rev.* **1980**, *108*, 1279-1292.
37. Petersen, R.A.; Stackpole, J.D. Overview of the NMC Production Suite; *Wea. Forecasting* **1989**, *4*, 313-322.
38. Stunder, B.J.B. NCEP Model Output—FNL Archive Data; National Climatic Data Center (NCDC) Report TD-6141; National Climatic Data Center: Washington, DC, 1997.
39. Seibert, P.; Frank, A. Source-Receptor Matrix Calculation with a Lagrangian Particle Dispersion Model in Backward Mode; *Atmos. Chem. Phys. Discuss.* **2003**, *3*, 4516-4548.
40. Desiato, F.; Anfossi, D.; Castelli, S.T.; Ferrero, E.; Tinarelli, G. The Role of Wind Field, Mixing Height and Horizontal Diffusivity Investigated through Two Lagrangian Particle Models; *Atmos. Env.* **1998**, *32*, 4157-4165.
41. Zannetti, P. *Air Pollution Modeling*; Computational Mechanics Publications: Southampton Boston, MA, 1990.
42. Pitchford, M.; Pitchford, A. Analysis of Regional Visibility in the Southwest Using Principal Component and Back Trajectory Techniques; *Atmos. Env.* **1985**, *19*, 1301-1316.
43. Iyer, H.K.; Malm, W.C.; Ahlbrandt, R.A. A Mass Balance Method for Estimating the Fractional Contribution from Various Sources to a Receptor Site; In *Transactions: Visibility Protection: Research and Policy Aspects*; Bhardwaja, P.S., Ed.; Air Pollution Control Association: Grand Teton National Park, WY, Pittsburgh, PA, 1986; pp 861-869.
44. Gebhart, K.A.; Schichtel, B.A.; Barna, M.G. Source Apportionment of Sulfate and Unique Tracers at Big Bend National Park Using a Back-Trajectory Based Receptor Model and Measurements from the BRAVO Study; Presented at the Air & Waste Management Association's 96th Annual Meeting & Exhibition, San Diego, CA, June 2003.
45. Belsley, D.A.; Kuh, E.; R.E. Welsch, R.E. *Regression Diagnostics—Identifying Influential Data and Sources of Collinearity*; John Wiley & Sons: New York, NY, 1980; pp 92-93.
46. Kahl, J.D.; Harris, J.M.; Herbert, G.A. Intercomparison of Three Long-Range Trajectory Models Applied to Arctic Haze. *Tellus* **1989**, *41B*, 524-536.

About the Authors

Kristi A. Gebhart, research physical scientist, Bret A. Schichtel, physical scientist, and Michael G. Barna, physical scientist are with the National Park Service, Air Resources Division, Cooperative Institute for Research in the Atmosphere. Address correspondence to: Kristi A. Gebhart, National Park Service, Air Resources Division, Cooperative Institute for Research in the Atmosphere, Colorado State University, Fort Collins, CO 80523; phone: +1-970-491-3684; fax: +1-970-491-8598; e-mail: gebhart@cira.colostate.edu.